Molecular Crystals and Liquid Crystals
Publication details, including instructions for authors and subscription information:
http://www.tandfonline.com/loi/gmcl20

Analysis of Bone in Rats of End Stage Kidney Disease by Vibrational Spectroscopy

H. Kimura-Suda [a], M. Kuwahara [b], K. Hidaka [a], K. Kanazawa [a], K. Honma [a], H. Ueno [a], K. Bannai [b], M. Sugano [b], M. Kajiwara [c], A. Ohnishi [d] & H. Yamato [b]

[a] Department of Bio- and Material Photonics, Chitose Institute of Science and Technology, 758-65 Bibi, Chitose, Hokkaido, 066-8655, Japan

[b] Kureha Corporation, 3-26-2 Hyakunin-cho Shinjyuku-ku, Tokyo, 169-8503, Japan

[c] Kureha Special Laboratory Co. Ltd., 3-26-2 Hyakunin-cho Shinjyuku-ku, Tokyo, 169-8503 Japan

[d] Perkin Elmer Japan, 134 Godocho, Hodogaya, Yokohama, 240-0005, Japan

Version of record first published: 12 Sep 2012.

To cite this article: H. Kimura-Suda , M. Kuwahara , K. Hidaka , K. Kanazawa , K. Honma , H. Ueno , K. Bannai , M. Sugano , M. Kajiwara , A. Ohnishi & H. Yamato (2012): Analysis of Bone in Rats of End Stage Kidney Disease by Vibrational Spectroscopy, Molecular Crystals and Liquid Crystals, 566:1, 75-79

To link to this article: http://dx.doi.org/10.1080/15421406.2012.701831

Mol. Cryst. Liq. Cryst., Vol. 566: pp. 75–79, 2012

ISSN: 1542-1406 print/1563-5287 online
DOI: 10.1080/15421406.2012.701831

Taylor & Francis
Taylor & Francis Group

Analysis of Bone in Rats of End Stage Kidney Disease by Vibrational Spectroscopy

H. KIMURA-SUDA,[1,*] M. KUWAHARA,[2] K. HIDAKA,[1] K. KANAZAWA,[1] K. HONMA,[1] H. UENO,[1] K. BANNAI,[2] M. SUGANO,[2] M. KAJIWARA,[3] A. OHNISHI,[4] AND H. YAMATO[2]

[1]Department of Bio- and Material Photonics, Chitose Institute of Science and Technology, 758-65 Bibi, Chitose, Hokkaido 066-8655, Japan
[2]Kureha Corporation, 3-26-2 Hyakunin-cho Shinjyuku-ku, Tokyo 169-8503, Japan
[3]Kureha Special Laboratory Co. Ltd., 3-26-2 Hyakunin-cho Shinjyuku-ku, Tokyo 169-8503 Japan
[4]Perkin Elmer Japan, 134 Godocho, Hodogaya, Yokohama 240-0005, Japan

End stage kidney disease (ESKD) patients are characterized to reduce bone strength due to disordering of calcium and phosphorous homeostasis. We demonstrate the use of Fourier transform infrared imaging and Raman spectroscopy to characterize bone quality in ESKD rats. Eleven-week male rats treated 5/6-nephrectomy and sham-operated rats were kept for 16 weeks, and then each femur was removed for measurements. We observe excess bone resorption compared to bone formation in ESKD rat, and bone mineral loss in endosteum is observed rather than in periosteum. We also find trabecular bone and epiphysis have a rapid turnover rate compared to cortical bone.

Keywords FTIR imaging; bone; kidney; Raman; hydroxylapatite; collagen

Introduction

Kidney has several important roles physiologically: removing waste products from the blood, regulating the water fluid levels, and maintaining calcium and phosphorous homeostasis (Figure 1) [1]. Gradual loss of kidney function, which is called chronic kidney disease (CKD), leads to high level of wastes in blood, high blood pressure, and calcium and phosphorous homeostasis disorder. Bone consists of about 45–70 wt% mineral formed mostly of calcium phosphate (hydroxylapatite), 10wt% water, and the remainder organic matrix consisting principally type I collagen with smaller amounts of noncollagenous proteins and lipids [2]; accordingly, calcium and phosphorous homeostasis disorder causes mineral and bone disorder (MBD), what is called CKD-MBD [3–4]. The stages of CKD are mainly based on measured or estimated GFR (Glomerular Filtration Rate), which is estimated from creatinine clearance rate (CCr) [1]. There are five stages but kidney function

*Address correspondence to H. Kimura-Suda +81-123-27-6008. E-mail: kimurasu@photon.chitose.ac.jp

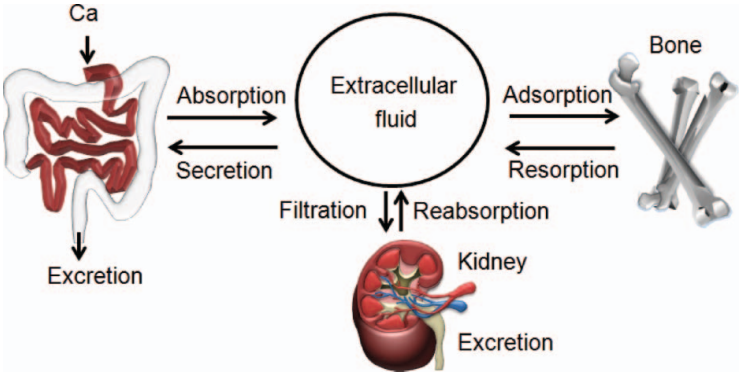

Figure 1. Pathways leading to calcium homeostasis in the organism.

is normal in Stage 1. End stage kidney disease (ESKD), stage 5, patients are characterized to be getting GFR under 15 and reduce bone strength, which reflects bone mineral density and bone quality. Bone quality is defined by at least four factors: (1) the rate of bone turnover; (2) properties of the mineral/collagen matrix; (3) microdamage accumulations; (4) architecture/geometry of trabecula and cortical bone [5]. The secondary osteoporosis arises regardless of age or sex and results from underlying specific disease such as secondary hyperparathyroidism due to CKD [6], and it is difficult to treat rather than primary osteoporosis such as postmenopausal and age-related involutional osteoporosis.

Vibrational spectroscopy such as Fourier transform infrared (FTIR) [7–9] and Raman spectroscopy [10–12] is simple but a powerful tool for both qualitative and quantitative analysis of materials without homogenization. FTIR imaging system, provides data with distribution of functional groups, has come to be available for pathphysiological elucidation in mediobiological [7–9]. We previously characterized bone quality of mouse in rickets by FTIR imaging, and successes in visualization of both bone density and quality [9]. In this paper, we describe the complementary analysis by FTIR imaging system and Raman spectroscopy to characterize bone quality of femurs in rats with ESKD.

Experiment

Eleven week-old male rats underwent 5/6 subtotal nephrectomy (Nx), and sham operated rats (Sham) were kept for 16 weeks. Biochemical markers of serum and urine were measured

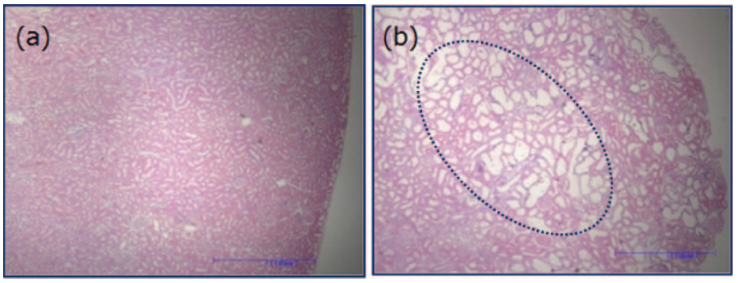

Figure 2. Cross section of kidney in Sham rat (a) and 5/6-Nx rat (b) stained in hematoxylin-eosin (HE). The area in the dotted circle in (b) shows tissue destroyed by kidney hypertrophy.

due to calculate CCr to make sure of being CKD. After sacrifice, each femur was removed, and then fixed with 70% ethanol. Then femurs were embedded in PMMA, and cut into two to make longitudinal sections for Raman measurement. All longitudinal sections were sliced into 3 μm by microtome and mounted on BaF_2 disks for FTIR imaging measurements.

FTIR imaging system with a mercury-cadmium-telluride (MCT) linear array detector (Spotlight400 system, PerkinElmer, MA USA) was used to characterize the longitudinal sections. FTIR images were recorded over the range 4000–680 cm^{-1}, using a transmittance mode, a resolution of 8 cm^{-1}, an accumulated number of 2 times, and a pixel size of 25 μm^2.

The longitudinal sections were also characterized by Raman (EMS-310 photondesign, Japan) with a standard fluorescence microscope. Laser light of 1064nm Nd:YAG producing laser power ~40 mW was focused on the sample through a 18 x /0.4NA objective. Raman signals were collected in 3 scans of 3 minutes for diaphysis and 10 scans of 3 minutes for

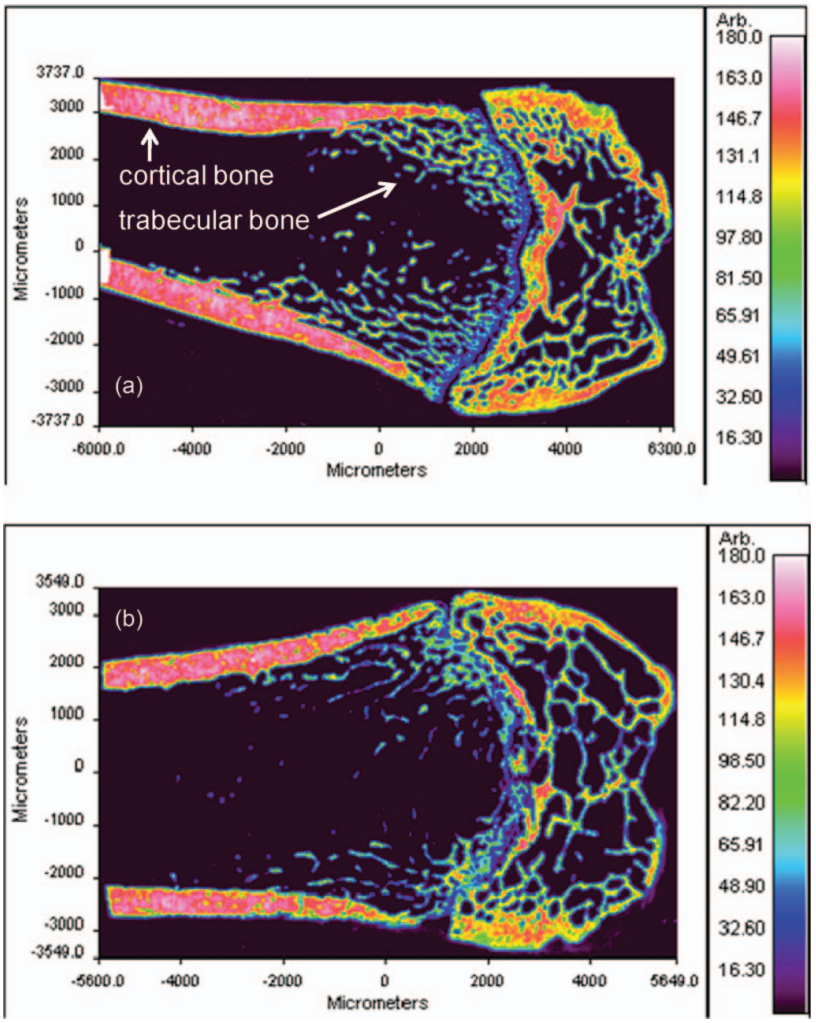

Figure 3. FTIR images showing distribution of phosphate (PO_4^{3-}) in longitudinal sections of femurs in Sham rat (a) and ESKD rat (b).

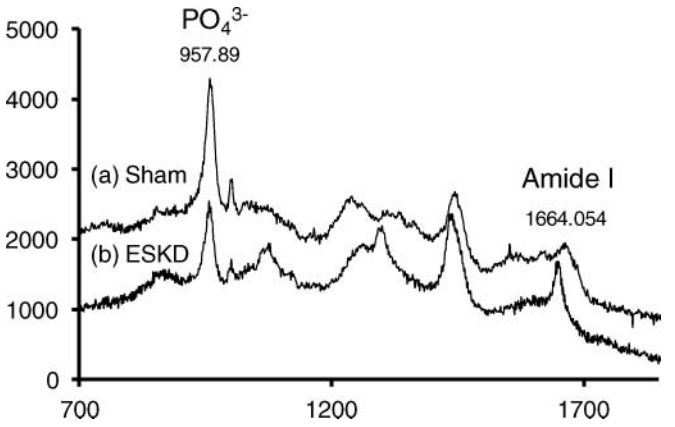

Figure 4. Raman spectra of trabecular bone in femurs in Sham rat (a) and ESKD rat (b).

epiphysis, with an InGaAs detector, in the spectral interval from 255 to 1925 cm^{-1}, with a resolution of 4 cm^{-1}.

Results and Discussion

We prepared 5/6-Nx rats to make a model of ESKD rats. The 5/6-Nx rat has commonly been used as an experimental model for CKD in human. Figure 2 shows cross section of kidney stained in hematoxyline-eosine: (a) Sham and (b) 5/6-Nx rat. Kidney hypertrophy is observed in 5/6-Nx rat, and then excess fibrous tissue destroys the structure of kidney. We determined CCr to make sure of being CKD, and the value of CCr of Sham and 5/6-Nx rat after 16 weeks were 2.86 mL/min and 0.47 mL/min, respectively. These results indicate the kidney function in 5/6-Nx rat is low level as much as ESKD patient.

Figure 3 shows FTIR images of phosphate (PO_4^{3-}) band delivered from hydroxylapatite in longitudinal sections of femurs. Color scale showing distribution of PO_4^3 band in FTIR image was used to characterize bone mineral density. In the FTIR image of ESKD

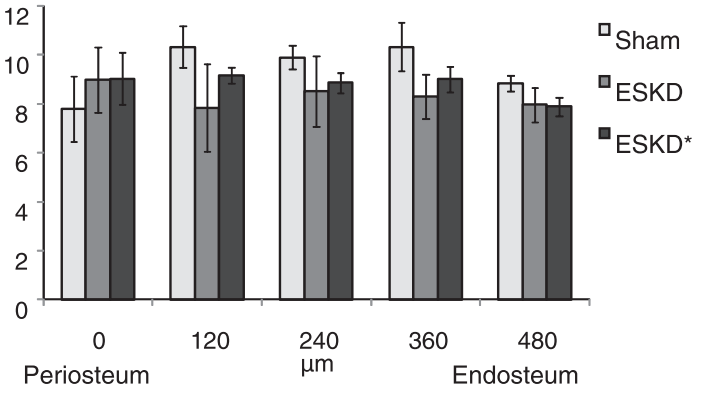

Figure 5. Histogram displaying the average of mineral/collagen matrix ratios in cortical bone in femurs. Sham rat (white), ESKD rat (gray), ESKD* (dark gray). ESKD* rat died at 16 weeks, after it underwent 5/6-Nx.

rat, rapid bone loss is observed in trabecular bone and epiphysis rather than cortical bone. This result means that trabecular bone and epiphysis have a rapid turnover rate rather than cortical bone. Raman spectra of trabecular bone (Figure 4) also indicate that the height of PO_4^{3-} band to the height of amide I band in the spectrum of ESKD is lower than that of Sham.

Raman analysis is used to find out the differences in cortical bone between Sham and ESKD rats. Figure 5 shows histogram displaying the average of mineral/collagen matrix ratios in the cortical bone of Sham, ESKD and ESKD*. Here, ESKD* is the rat died during 16 weeks after underwent 5/6-Nx. The mineral/collagen matrix ratio is a measure of the mineral content, and it is calculated as the ratio of the height of the PO_4^{3-} band to the height of the amide I band in Raman spectrum. Each data was averaged in five Raman measurements. In ESKD and ESKD* rats, mineral/collagen matrix ratios in the cortical bone show bone mineral loss is slightly observed in endosteum rather than in periosteum.

FTIR images of longitudinal sections of femurs revealed the distribution hydroxylapatite in wide area, and Raman analysis revered mineral/collagen matrix ratio in small area of bone. Both FTIR and Raman spectroscopies were useful to characterize bone quality and quantity rather than other conventional methods in medical and pharmaceutical fields because of FTIR and Raman data including information of chemical structure.

Conclusion

We reported that FTIR and Raman spectroscopies were extremely useful tool for evaluation of bone quality in ESKD for the first time. That is to say, we could show as component-imaging the differences between endosteal and periosteal quality and bone metabolism. We expect that FTIR and Raman might become strategic equipments for not only bone biology but also other life sciences.

References

[1] Guyton, A. G. and Hall, J. E. (2010). *Textbook of Medical Physology 11th Edition*, Elsevier Japan: Japan.
[2] H. Skinner (2005). *Biominerals Mineralogical Mag*., *69*, 621.
[3] Iwasaki-Ishizuka, Y., Yamato, H., Nii-Kono, T., Kurokawa, K. and Fukagawa, M. (2005). *Nephrol Dial Transplant*, *20*, 1904.
[4] Moe, S. M., Chen, N. X., Seifert, M. F., Sinders, R. M., Duan, D., Chen, X., Liang, Y., Radcliff, J. S., White, K. E. and II, V. H. G. (2009). *Kidney Int.*, *75*, 176.
[5] Burr, D. B. (2004). *J Musculoskel Neuron Interact*, *4*, 184.
[6] Bartl, R. and frisch, B. (2009). *Osteoporosis: Diagnosis, Prevention, Therapy Second Edition*, Springer-Verlag: Berlin Heidelberg, Germany.
[7] Boskey, A. and Camacho, N. P. (2007). *Biomaterilas*, *28*, 2465.
[8] Pleshko, N., Boskey, A. and Mendelsohn, R. (1991). *Biophys J.*, *60*, 786.
[9] Kimura-Suda, H., Kajiwara, M., Matsumoto, N., Murayama, H. and Yamato, H. (2009). *Mol. Cryst. Liq. Cryst.*, *505*, 64.
[10] Timlin, J. A., Carden, A. and D. Morris, M. (2000). *Anal. Chem.*, *72*, 2229.
[11] Tarnowski, C. P., Ignelzi, M. A. JR and Morris, M. D. (2002). *J Bone Miner Res*, *17*, 1118.
[12] Crane, N. J., Popescu, V., Morris, M. D., Steenhuis, P. and Ignelzi, M. A. JR (2006). *Bone*, *39*, 434.